Full Paper

Electrochemical Oxidation of Metolazone at a Glassy Carbon Electrode

A. Dora R. Pontinha, S. Carlos B. Oliveira, Ana Maria Oliveira-Brett*

Departamento de Química, Faculdade de Ciências e Tecnologia, Universidade de Coimbra, 3004-535 Coimbra, Portugal
*e-mail: brett@ci.uc.pt

Abstract
Metolazone is a diuretic agent used in patients with edematous states and/or hypertension. The electrochemical behavior of metolazone on a glassy carbon electrode was investigated using cyclic, differential pulse, and square-wave voltammetry at different pHs. The pH dependent oxidation of metolazone occurs in two consecutive steps in a diffusion-controlled mechanism and involves the formation of a main oxidation product. The first oxidation process is reversible, and involves two electrons and two protons corresponding to the oxidation of nitrogen in the sulfonamide moiety. The second oxidation process is irreversible, also occurs in the sulfonamide moiety, involves a one electron-transfer, and is followed by deprotonation to produce a cation radical, which reacts with water and yields a hydroxylated product. The diffusion coefficient of metolazone was calculated to be 3.43×10^{-6} cm^2 s^{-1} in pH 7.0 0.1 M phosphate buffer.

Keywords: Metolazone, Electrochemistry, Voltammetry, Oxidation mechanism, Diffusion process

1. Introduction

Diuretics are widely used in the treatment of congestive heart failure and hypertension. The major indications for diuretics are the enhancement of renal excretion of salt and water and lowering of blood pressure. In addition, sodium cations and chloride anions may also affect the renal readsorption and excretion of potassium, calcium, magnesium and other ions. Some diuretics increase urinary potassium excretion and can cause hypokalemia in patients treated with these medications for prolonged times [1, 2].

Diuretics are usually classified according to their chemical structures and physicochemical properties into the following four different groups: thiazides (e.g., hydrochlorothiazide and bendroflumethiazide), loop diuretics (e.g., bumetanide and furosemide), potassium-sparing diuretics (e.g., amiloride and triamterene), and carbonic anhydrase inhibitors (e.g., acetazolamide). Based on the effect of diuresis, diuretics can also be classified into high-efficiency diuretics (such as loop diuretics), medium-efficiency diuretics (such as thiazides and related compounds) and low-efficiency diuretics (such as potassium-sparing diuretics and carbonic anhydrase inhibitors) [1].

Metolazone (MT) [7-chloro-1,2,3,4-tetrahydro-2-methyl-4-oxo-3-*O*-tolyl-6-quinazoline-sulfonamide] (Scheme 1) is structurally related to the quinazoline sulfonamide series of diuretic agents and is considered a relatively potent, long-acting diuretic and natriuretic agent with minimal kaliuretic activity. Many of its pharmacological properties are comparable to the thiazide group of diuretics. MT is generally

given orally and is absorbed quite readily in the gastro-intestinal tract. MT excretion is primarily by filtration and secretion in the kidney but a significant amount of the drug appears in the feces following usual therapeutic doses because of enterohepatic recycling. A single oral dose of MT is excreted in two to four days, with 50 % excreted unchanged. Metabolites of MT are mainly hydroxylated and then further oxidized by various mechanisms [3–7].

Different methods have been applied for the determination of MT in bulk and pharmaceutical preparations including, spectrophotometric, high-performance liquid chromatographic, liquid chromatography with fluorescence detection, liquid chromatography-tandem mass spectrometry (LC-MS-MS) and LC-MS-MS with an electrospray ionization [8–10]. However, more recently, there has been a tendency for the use of less costly techniques and a reduction in the use of organic solvents since they result in high ecological costs.

Due to their high sensitivity, voltammetric methods have been successfully used for the detection and determination
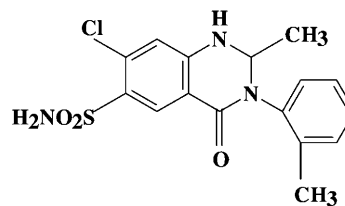
Scheme 1. Chemical structure of MT.

of various pharmaceutical compounds. Moreover, investigations of the redox behavior of pharmaceutical compounds by means of electrochemical techniques have the potential for providing valuable insights into the redox reactions of these molecules [11–16]. Nevertheless, there are no electrochemical studies of MT.

The present study is concerned with the electrochemical characterization of the oxidation behavior of MT, for a wide pH range between 2 and 12, using cyclic, square-wave and differential pulse voltammetry at a glassy carbon electrode.

2. Experimental

2.1. Materials and Reagents

Metolazone was obtained from Sigma and used without further purification. A stock solution of 66 μM MT was prepared in water and stored at 5 °C. Solutions of different concentrations of MT were prepared by dilution of the appropriate quantity in supporting electrolyte.

All supporting electrolyte solutions (Table 1) were prepared using analytical grade reagents and purified water from a Millipore Milli-Q system (conductivity ≤ 0.1 μS cm^{-1}).

Table 1. Supporting electrolytes, 0.2 M ionic strength.

pH	Composition
2.2	$HCl + KCl$
3.4	$HAcO + NaAcO$
4.5	$HAcO + NaAcO$
5.3	$HAcO + NaAcO$
6.1	$NaH_2PO_4 + Na_2HPO_4$
7.0	$NaH_2PO_4 + Na_2HPO_4$
8.1	$NaH_2PO_4 + Na_2HPO_4$
9.3	$NaOH + Na_2B_2O_7$
11.1	$NaOH + KCl$
12.8	$NaOH + KCl$

Microvolumes were measured using EP-10 and EP-100 Plus Motorized Microliter Pippettes (Rainin Instrument Co. Inc., Woburn, USA). The pH measurements were carried out with a Crison micropH 2001 pH-meter with an Ingold combined glass electrode. All experiments were done at room temperature ($25 \pm 1\,^{\circ}C$).

2.2. Voltammetric Parameters and Electrochemical Cells

Voltammetric experiments were carried out using a μAutolab running with GPES 4.9 software, Eco-Chemie, Utrecht, The Netherlands. Measurements were carried out using a glassy carbon electrode (GCE) ($d = 1.5$ mm) working electrode, a Pt wire counter electrode, and an Ag/AgCl (3 M KCl) as reference, in a 0.5 mL one-compartment electrochemical cell. The experimental conditions for differ-

ential pulse voltammetry were: pulse amplitude 50 mV, pulse width 70 ms, scan rate 5 mV s^{-1}. For square-wave voltammetry the experimental conditions were frequency 50 Hz and potential increment 2 mV, corresponding to an effective scan rate 100 mV s^{-1}.

The GCE was polished using diamond spray (particle size 1 μm) before every electrochemical assay. After polishing, the electrode was rinsed thoroughly with Milli-Q water. Following this mechanical treatment, the GCE was placed in buffer supporting electrolyte and differential pulse voltammograms were recorded until a steady state baseline voltammogram was obtained. This procedure ensured very reproducible experimental results.

2.3. Acquisition and Presentation of Voltammetric Data

The differential pulse voltammograms presented were background-subtracted and baseline-corrected using the moving average application with a step window of 5 mV included in GPES version 4.9 software. This mathematical treatment improves the visualization and identification of peaks over the baseline without introducing any artifact, although the peak intensity is in some cases reduced ($<10\%$) relative to that of the untreated curve. Nevertheless, this mathematical treatment of the original voltammograms was used in the presentation of all experimental voltammograms for a better and clearer identification of the peaks. The values for peak current presented in all plots were determined from the original untreated voltammograms after subtraction of the baseline.

3. Results and Discussion

3.1. Cyclic Voltammetry

The voltammetric behavior using a GCE was investigated in a solution of 30 μM MT in pH 7 0.1 M phosphate buffer saturated with N_2. The cyclic voltammograms obtained at a scan rate $\nu = 100$ mV s^{-1}, show two well-separated consecutive peaks in the anodic region (Fig. 1A), but no peaks were observed in the cathodic region.

The first oxidation is reversible (Fig. 1B), peaks $1_a - 1_c$, and the second oxidation, peak 2_a, at $E_{pa}^2 = +0.815$ V, corresponds to an irreversible reaction (Fig. 1A). The second scan shows the decrease of peak 2_a current and the absence of peak 1_a due MT and MT oxidation products adsorption on the GCE surface.

The effect of scan rate on peak 2_a current was studied (Fig. 2). Between measurements, the electrode surface was always polished in order to assure a clean surface and to avoid possible problems from MT and MT oxidation products absorption on the GCE surface.

It was observed that increasing the scan rate the peak 2_a potential is slightly displaced to more positive values. The difference between the peak 2_a potential, E_{pa}^2, and the peak 2_a potential at half height of peak, $E_{p/2a}^2$, is ca. 43 mV. Since
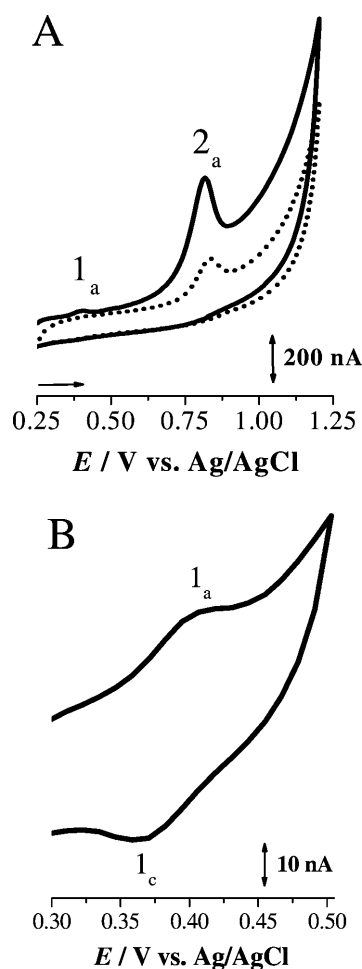
A

B

Fig. 1. Cyclic voltammograms of 30 μM MT in pH 7 0.1 M phosphate buffer: A) (—) first and (·····) second scan, and B) first peak, $v = 100$ mV s^{-1}.
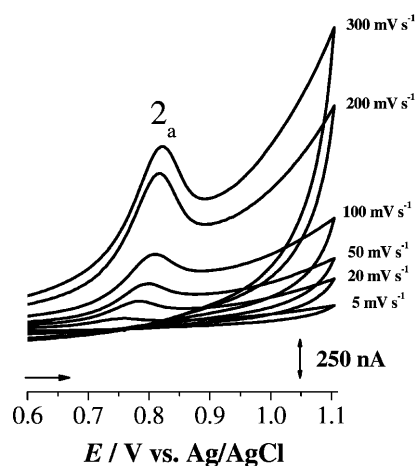

Fig. 2. Cyclic voltammograms of 30 μM MT in pH 7 0.1 M phosphate buffer at scan rates: 5, 20, 50, 100, 200, and 300 mV s^{-1}.

for a diffusion-controlled irreversible system $| E_{pa}^2 - E_{p/2a}^2 | = 47.7/(\alpha_a n')$ where α_a is the anodic charge transfer coefficient and n' the number of electrons in the rate-determining step [17], it can be calculated that $\alpha_a n' = 1.11$.

Increasing the scan rate, the current of peak 2_a increases linearly with square root of v, consistent with the diffusion-limited oxidation of a solution species.

The peak current in amperes for a diffusion-controlled irreversible system is given by I_{pa} (A) $= 2.99 \times 10^5 n (\alpha_a n')^{1/2} A [R]_\infty D_R^{1/2} v^{1/2}$ where n' is the number of electrons transferred during the oxidation of MT ($n' = 1$ as shown below, Sec. 3.2), A is the electrode area in cm^2, D_R is the diffusion coefficient of R in cm^2 s^{-1}, $[R]_\infty$ is the concentration in mol cm^{-3} and v is in V s^{-1} [17]. By plotting I_{pa} vs. $v^{1/2}$, the value of D_R is obtained. For this calculation, the GCE electroactive area was determined from a plot of I_{pc} vs. $v^{1/2}$ using a solution of 500 μM hexacyanoferrate (II) and the value of the diffusion coefficient of hexacyanoferrate (II) in phosphate buffer of 7.35×10^{-6} cm^2 s^{-1} [18], and the GCE electroactive area of 1.03×10^{-5} cm^2 was determined. For the measured slope of 3.72×10^{-8} A/(V s^{-1})$^{1/2}$ the diffusion coefficient of MT in pH 7 0.1 M phosphate buffer is 3.43×10^{-6} cm^2 s^{-1}.

3.2. The Influence of pH

The effect of pH on the electrochemical oxidation of MT was studied over a wide pH range between 2 and 12 using differential pulse voltammetry. The differential pulse voltammograms (Fig. 3) were all recorded in solutions of 30 μM MT in different electrolytes with 0.2 M ionic strength (Table 1).

The reversible peak 1_a only occurs in the pH range 2–10 and the oxidation potential was displaced to less positive values with increasing pH (Figs. 3A and C). In the E_{pa} vs. pH plot (Fig. 3C) the slope of the dotted line, 59 mV per pH unit, shows that the mechanism of this first reversible oxidation process, peaks 1_a–1_c, in aqueous media involves the same number of electrons and protons. Taking into consideration that width at half height of the MT peak 1_a is $W_{1/2} \approx 54$ mV, it can be concluded that this oxidation process involves the transfer of two electrons and two protons.

The peak 2_a occurs in all supporting electrolytes (Fig. 3A and C). For buffer solutions between pH 2 and 10, the potential of peak 2_a is displaced to more negative values with increasing pH. In the E_{pa} vs. pH plot (Fig. 3C) the slope of the dotted line, 59 mV per pH unit, shows that the mechanism of this oxidation process, Peak 2_a, in aqueous media also involves the same number of electrons and protons.

The number of electrons transferred, n, was determined by the peak width at half height $W_{1/2} \approx 100$ mV, and is close to the theoretical value of 90 mV, corresponding to an electrochemical reaction involving the transfer of one electron [17]. Consequently, it can be concluded that oxidation process occurs with the transfer of one electron and one proton.

For pH > 10, the oxidation peak 2_a does not depend on pH indicating a mechanism involving only 1 electron, the MT oxidation product can undergo chemical deprotonation in

A

B

C

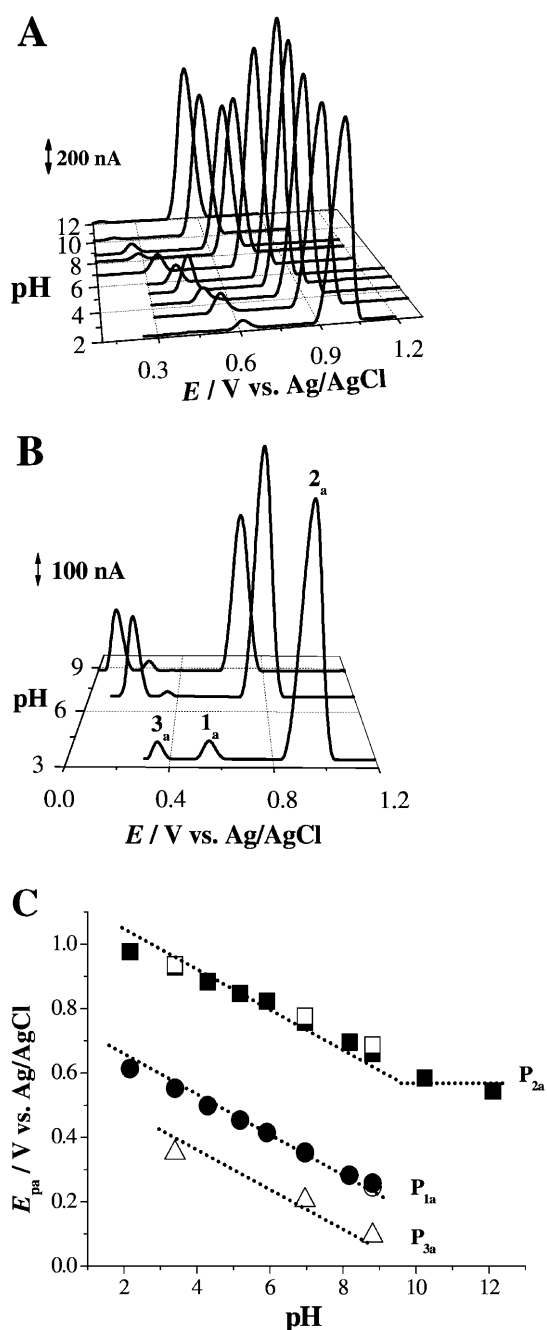

Fig. 3. 3D plots of background-subtracted differential pulse voltammograms obtained in 30 μM MT as a function of pH: A) first and B) second scans. C) Plot E_{pa} vs. pH of: (●) peak 1_a and (■) peak 2_a for the first and (●) peak 1_a, (□) peak 2_a and (△) peak 3_a for the second scans. Dotted line corresponds to 59 mV per pH unit.

alkaline electrolytes [19], and the value of $pK_a \approx 10$ of MT was determined (Fig. 3C).

Successive differential pulse voltammograms in buffer solutions with pH 3.5, 7.0 and 9.0 were recorded. For all these pHs a new peak 3_a occurs in the second differential pulse voltammogram (Fig. 3B) which corresponds to the oxidation of the MT oxidation product, and increasing the pH a decrease of the oxidation potential was observed

(Fig. 3B) and the slope of the dotted line, 59 mV per pH unit (Fig. 3C) shows that the mechanism of this oxidation process, Peak 3_a, in aqueous media also involves the same number of electrons and protons.

The variation of peak 2_a current versus pH showed that the current increased with pH (Fig. 3A), with a maximum in the pH range 6–7 using 0.1 M phosphate buffer, and this electrolyte was used for further studies.

3.3. Square-Wave Voltammetry

The advantages of square-wave voltammetry are greater speed of analysis, lower consumption of the electroactive species in relation with differential pulse voltammetry, and reduced problems with poisoning of the electrode surface [17]. A greater advantage of square-wave voltammetry is the possibility to see during only one scan if the electron transfer reaction is reversible or not. Since the current is sampled in both positive and negative-going pulses, peaks corresponding to the oxidation and reduction of the electroactive species at the electrode surface can be obtained in the same experiment.

Successive square-wave voltammograms recorded in a solution of 30 μM MT in different electrolytes showed similar features to the differential pulse voltammograms, i.e., oxidation peaks 1_a, 2_a, and 3_a. Consequently, the reversibility of the peaks 1_a and 3_a and the irreversibility of the peak 2_a were confirmed by plotting the forward and backward components of the total current obtained in a solution of MT in pH 7 0.1 M phosphate buffer (Fig. 4).

Based on the results obtained a mechanism for the oxidation of MT in pH 7 0.1 M phosphate buffer is proposed (Scheme 2), which is in agreement with the MT data obtained using other methodologies [3, 11, 20, 21]. The first step, peak 1_a, is assigned to the oxidation of the nitrogen in the sulfonamide moiety and involves the transfer of two electrons and two protons. The second step occurs also in the sulfonamide moiety, peak 2_a, and involves one electron-transfer, followed by deprotonation to produce a cation radical, which reacts with water and yields the final hydroxylated product.
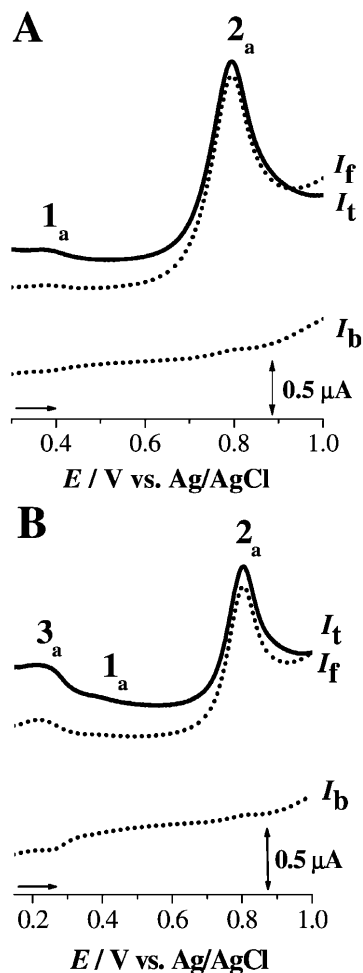
4. Conclusions

MT, a diuretic agent used in patients with edematous states and/or hypertension, undergoes oxidation at a glassy carbon electrode. The oxidation of MT occurs in two consecutive steps in a diffusion-controlled mechanism. The diffusion coefficient of MT in pH 7.0 0.1 M phosphate buffer was calculated to be 3.43×10^{-6} cm^2 s^{-1}.

The first oxidation process is reversible, pH dependent and involves the oxidation of nitrogen in the sulfonamide moiety with the transfer of two electrons and two protons. The second oxidation process occurs also in the sulfonamide moiety is irreversible, pH dependent, and involves one electron and one proton transfer to produce a cation radical,

Peak 1a

-2e -2H+

+2e +2H+

Peak 2a

-1e -1H+

H_2O
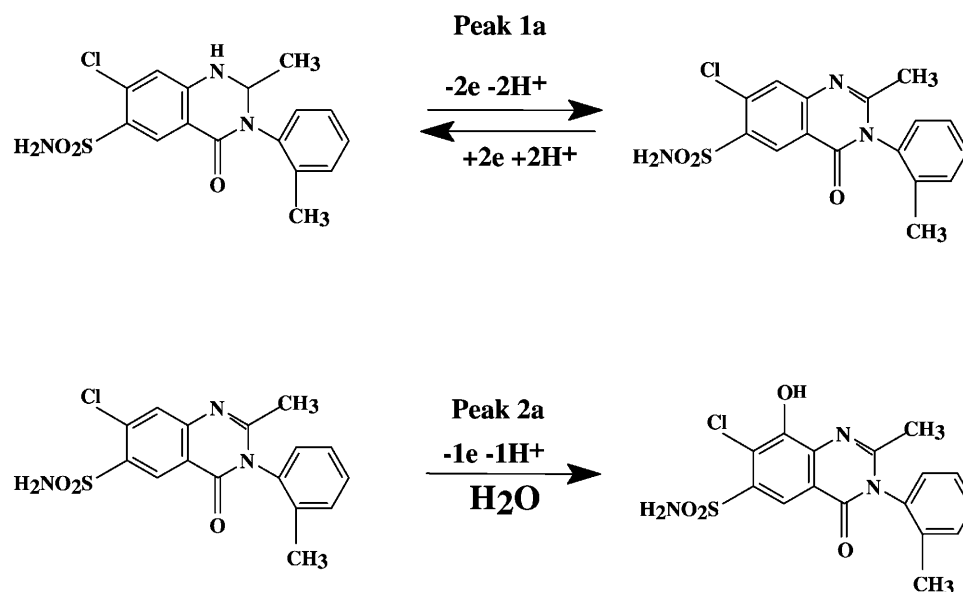
Scheme 2. Proposed oxidation mechanism of MT in pH 7.

which reacts with water and yields a final hydroxylated product.

5. Acknowledgements

6. References

[1] M. H. Lu, P. Tong, H. Xiao, S. F. Xia, X. Y. Zheng, W. Liu, L. Zhang, G. N. Chen, *Electrophoresis* **2007**, *28*, 1461.
[2] B. J. Materson, *J. Am. Chem. Soc. Hypertens.* **2007**, *1*, 373.
[3] A. Stern, *Am. Heart J.* **1976**, *91*, 262.
[4] Steinmul.Sr, J. B. Puschett, *Kidney Int.* **1972**, *1*, 169.
[5] K. Mohammad, W. David, S. J. Enna, B. B. David, in *xPharm: The Comprehensive Pharmacology Reference*, Elsevier, New York **2008**.
[6] J. F. Winchester, R. J. Kellett, K. Boddy, P. Boyle, H. J. Dargie, M. E. Mahaffey, D. M. Ward, A. C. Kennedy, *Clin. Pharmacol. Ther.* **1980**, *28*, 611.
[7] C. L. Curry, S. M. Janda, R. Harris, J. H. Mackay, C. A. Nugent, J. Ryan, H. Schnaper, J. Schoenberger, *Clin. Ther.* **1986**, *9*, 47.
[8] M. Ciborowski, M. C. Icardo, J. V. G. Mateo, J. Martínez Calatayud, *J. Pharm. Biomed.* **2004**, *36*, 693.
[9] D. Farthing, D. A. Sica, I. Fakhry, T. W. B. Gehr, *J. Chromatogr. B* **1994**, *653*, 171.
[10] G. Wei, S. Xiao, C. Liu, *J. Chromatogr. B* **2007**, *845*, 169.
[11] O. Abdel Razak, *J. Pharm. Biomed.* **2004**, *34*, 433.
[12] V. C. Diculescu, S. Kumbhat, A. M. Oliveira-Brett, *Anal. Chim. Acta* **2006**, *575*, 190.

Fig. 4. Square-wave voltammogram of 30 μM MT in pH 7 0.1 M phosphate buffer: A) first and B) second scan; I_t: total, I_f: forward and I_b: backward; $\nu_{effective} = 100$ mV s^{-1}.

[13] V. C. Diculescu, T. A. Enache, A. M. Oliveira-Brett, *Anal. Lett.* **2007**, *40*, 2860.

[14] M. Macher, R. Wintersteiger, *J. Chromatogr. B* **1995**, *709*, 257.

[15] R. T. Kachoosangi, G. G. Wildgoose, R. G. Compton, *Anal. Chim. Acta* **2008**, *618*, 54.

[16] S. A. Ozkan, B. Uslu, H. Y. Aboul-Enein, *Crit. Rev. Anal. Chem.* **2003**, *33*, 155.

[17] C. M. A. Brett, A. M. Oliveira Brett, *Electrochemistry: Principles, Methods and Aplications*, Oxford Science University Publications, Oxford **1993**.

[18] http://www.hbcpnetbase.com/, Handbook of Chemistry and Physics

[19] S. C. B. Oliveira, V. C. Diculescu, G. Palleschi, D. Compagnone, A. M. Oliveira-Brett, *Anal. Chim. Acta* **2007**, *588*, 283.

[20] A. I. Cohen, A. D. Hartman, O. N. Hinsvark, P. F. Kraus, W. Zazulak, *J. Pharm. Sci.* **1973**, *62*, 931.

[21] E. J. Belair, J. Yelnosky, A. I. Cohen, *Br. J. Pharmacol.* **1972**, *45*, 476.